Title
Physical modeling of the thermal-hydro-mechanical response of a thermally active soil-geosynthetic system

ISBN
9783981395396

Authors
Stewart, MA
Coccia, CJR
McCartney, JS

Publication Date
2014

Physical Modeling of the Thermal-Hydro-Mechanical Response of a Thermally Active Soil-Geosynthetic System

Melissa A. Stewart, Charles .J.R. Coccia & John S. McCartney

University of Colorado Boulder, Colorado, USA

ABSTRACT: This study involves the use of physical modeling to investigate the thermo-hydro-mechanical response of a thermally active soil-geosynthetic system. Specifically, load-settlement tests were performed on layers of compacted, unsaturated silt with a woven polypropylene geosynthetic embedded at mid-height before and after application of heat to the base of the soil layers. Changes in temperature and relative humidity at the soil layer boundaries were monitored during heating, while dielectric sensors embedded in the soil layer are used to monitor the temperature and water content with depth. Comparison of the load-settlement curves measured under ambient and elevated temperatures indicate an increase in stiffness of the overall system due to heating. This indicates that the impact of thermally induced water flow has a greater positive effect on the mechanical response of the soil-geosynthetic system than the negative effect of thermal softening of the geosynthetic.

Keywords: Soil-geosynthetic interaction, unsaturated soil, thermally active geotechnical systems

1 INTRODUCTION

Mechanically-stabilized earth (MSE) walls consist of alternating layers of compacted soil backfill and geosynthetic reinforcements. These composite systems allow for the mobilization of both tensile and compressive resisting forces to withstand self-weight and external loads. Although the mobilized resistance of these structures results from the shear strength of the soil, the tensile strength of the geosynthetic, and soil-geosynthetic interaction, the performance of MSE walls has been shown to be directly related to the stress state of the soil backfill. To avoid effects of pore water pressure on the stress state of the soil backfill, most design codes require freely draining backfills. As the cost and availability of freely draining backfills can be prohibitive for some projects, the use of poorly draining backfills have been evaluated (Zornberg and Mitchell 1994, Zornberg et al. 1995).

Although the performance of MSE walls with poorly draining backfills has been shown to be adequate, there is still some concern over their deformation response due to the effects of infiltration of water and slow rates of drainage. Increases in pore water pressure or degree of saturation that may occur in poorly draining backfills will lead to decreases in effective stress (Lu et al. 2010). A proposed method that is being investigated for control of the stress state in poorly draining backfills is the incorporation of geothermal heat exchangers within the reinforced soil mass (Stewart and McCartney 2013, Stewart et al. 2014). In this case, thermally induced water flow is expected to occur in the unsaturated soil away from the heat exchangers, leading to a lower degree of saturation, increased suction, and increased effective stress (Coccia and McCartney 2013). This soil improvement technique has the added advantage that MSE walls could be used to dissipate excess heat from power plants or buildings, making these systems more environmentally friendly and potentially less expensive.

Despite the potential positive effects of thermally induced water flow on the strength and stiffness of the reinforced soil mass, studies on geosynthetics indicates that there may be negative effects of temperature on the stress-strain response of reinforcing geosynthetics (Zornberg et al. 2004, Bueno et al. 2005, Karademir 2011). Therefore, it is important to consider whether the positive influence of a decreased degree of saturation in the soil offsets the negative aspects of thermal softening of the geosynthetic. The objective of this study is to evaluate the thermo-hydro-mechanical response of a soil-geosynthetic system by performing load-settlement tests on a model MSE wall layer made up of a woven polypropylene reinforcing geosynthetic embedded in a compacted unsaturated silt layer.

2 BACKGROUND

2.1 *Thermal Effects on Unsaturated Soils*

The thermo-mechanical response of unsaturated soil is dependent on the degree of saturation (Coccia and McCartney 2013) as well as the stress history. Heating of unsaturated soil may cause elasto-plastic volume changes which can be either expansive or contractive depending on the stress history of the soil (Uchaipichat and Khalili 2009). Normally consolidated to lightly overconsolidated soils will contract plastically due to the dissipation of thermally induced excess pore water pressure, while over-consolidated soils with overconsolidation ratios greater than 1.5 to 3 tend to exhibit elastic thermal expansion. Thermally induced water flow will result from the increase in temperature within an unsaturated soil mass. Water in both liquid and vapor phases will move from zones of high energy (higher temperatures) to low energy (lower temperatures). The extent to which water content is affected by temperature changes is largely a function of the initial soil properties, such as porosity, degree of saturation, and hydraulic conductivity (Thomas et al. 1996). As water flows out of the zone of higher temperature, the degree of saturation decreases, which can be directly related to an increase in suction through the soil-water retention curve (SWRC).

Coccia et al. (2012) evaluated the mechanical response of a compacted, unreinforced layer of Bonny silt at various temperatures. The silt layer had a thickness of 30.5 cm and was heated to different temperatures using a flexible heat exchanger embedded at mid-depth. Once the soil mass reached thermal and hydraulic equilibrium, a vertical load was applied to a plate at the top boundary of the soil and the deformation response of the soil was measured. The soil settled by 1.26 mm during an increase in temperature at mid-depth from 20 to 53 °C (Fig. 1a). During cooling, the soil layer settled an additional 0.3 mm. The stiffness of the soil layer increased with increasing temperature. In addition, the soil was observed to maintain an increased value of stiffness following cooling (Fig. 1b).

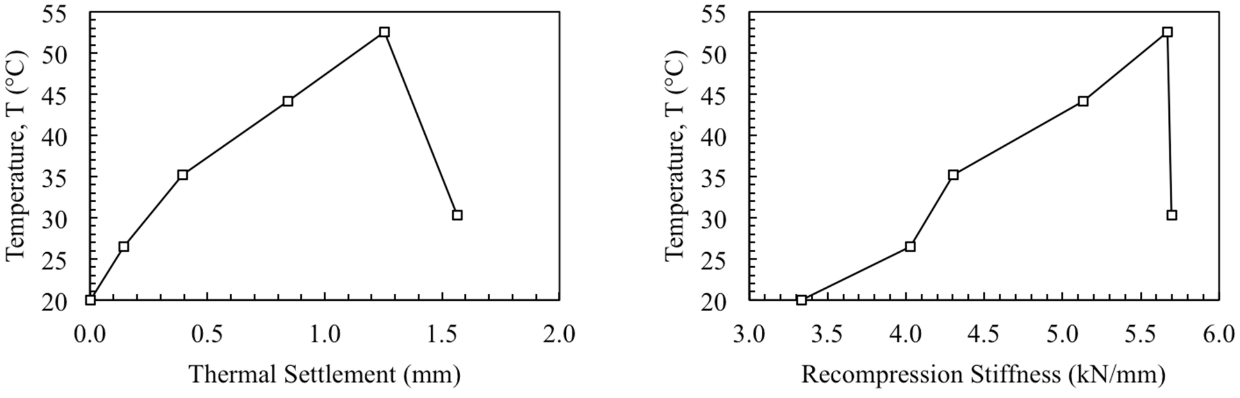

(a) (b)

Figure 1. Response of an unsaturated soil layer during application of elevated temperatures to an embedded heat exchanger at mid-height (Coccia et al. 2012): (a) Thermal settlement of the soil layer surface; (b) Change in recompression stiffness

2.2 *Thermal Effects on Geosynthetics*

In the effort to accelerate the time required for obtain creep data for various geosynthetics, several studies have evaluated the non-isothermal behavior of these materials (Zornberg et al. 2004, Bueno et al. 2005, Karademir 2011). These studies found that some geosynthetic polymers are susceptible to changes in stiffness at elevated temperatures. The most important property governing the thermal response of a polymer is the glass transition temperature (T_g), defined as the temperature at which the polymer shows a reduction in tensile stiffness or ceases to behave as a brittle material. Two common polymers used in geosynthetics are polyethylene terephthalate (PET) and polypropylene (PP) which have values of T_g of 70°C and 0°C, respectively. Generally, the stiffness of a polymer is unaffected by changes in temperature until the temperature of the polymer approaches or exceeds T_g. As such, PET based geosynthetics are expected to maintain their original stiffness up to 70 °C. However, PP is much more susceptible to temperature changes, with thermal softening occurring at small changes from ambient temperature. An analysis of the magnitude of thermal softening was performed by Stewart et al. (2014).

3 MATERIALS AND METHODS

3.1 *Testing Apparatus*

The container of Coccia et al. (2012) was used to investigate the thermo-hydro-mechanical response of reinforced unsaturated silt [Fig. 2]. The container has a depth of 381 mm, a width of 305 mm, and a length of 762. A 228.6 mm-thick layer of coarse, wetted gravel was first placed in the container to provide a rigid, free-draining bottom boundary condition. A soil layer having a thickness of 152.4 mm was then compacted atop the gravel.

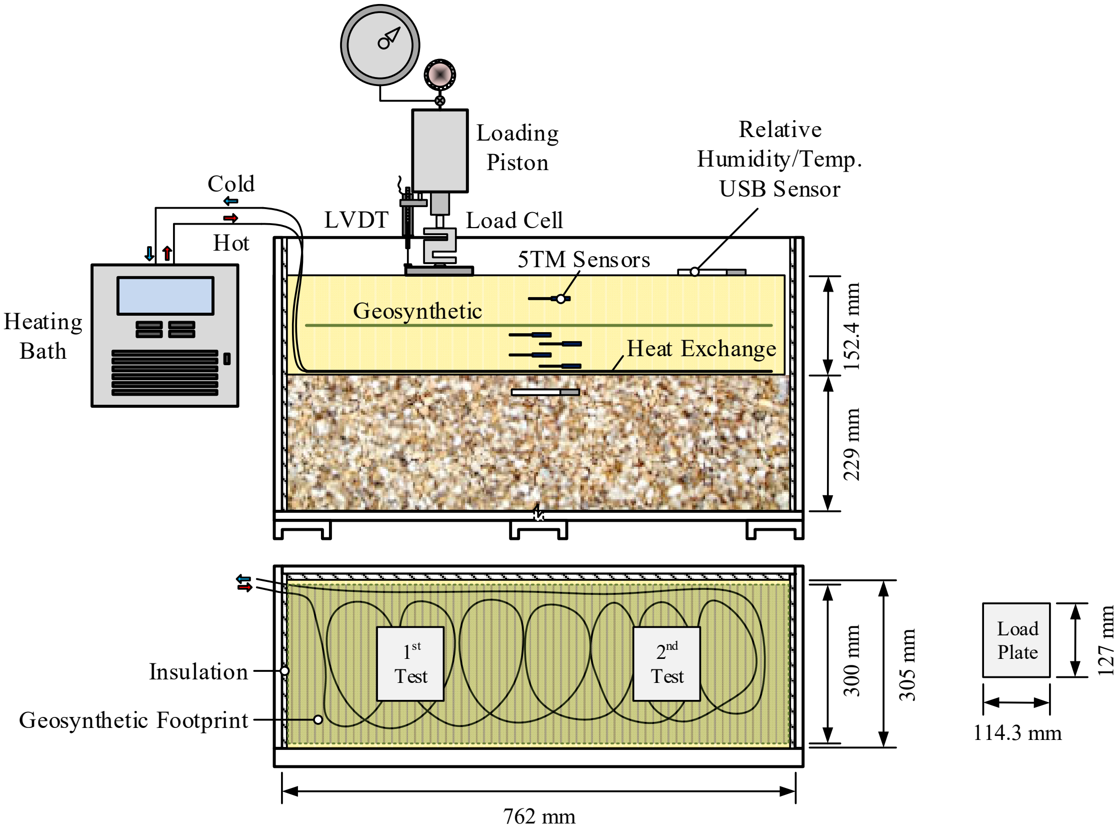

Figure 2: Schematic of testing apparatus labeled with instrumentation, load application mechanism and heat control system

A Lascar Electronics EL-USB-2-LCD temperature and humidity logger was placed within the gravel layer at the bottom boundary of the soil column to measure the bottom boundary condition for the soil layer. An additional EL-USB-2-LCD logger was placed on the soil surface to measure the top boundary condition for the soil layer. In order to evaluate changes in volumetric water content (VWC) and temperature (T) within the soil mass during heat injection, 5 Decagon 5-TE dielectric sensors were embedded in the soil layer at the depths listed in Table 1. A temperature correction was applied to the volumetric water content measurements as follows: $VWC = VWC_{measured} - 0.001725\Delta T$.

Table 1: Summary of depths of Decagon 5-TE sensors for each test

Test	Probe 1 (mm)	Probe 2 (mm)	Probe 3 (mm)	Probe 4 (mm)	Probe 5 (mm)
WPP-50C	38	76	114	152	152
WPP-45C	38	95	114	133	152

3.2 *Load and Temperature Control*

Load tests were performed on the surface of the soil layer by applying vertical loads to an aluminum plate that is 25.4 mm-thick by 127 mm-long by 114.3 mm-wide. The load was applied using a Bellofram pneumatic air cylinder mounted to a mobile frame that uses the box as a reaction. The vertical load was measured using a Futek LSB350 load cell having a capacity of 9.9 kN, while the corresponding settlement is measured using a DC linear variable differential transformer (LVDT) (model DC-EC-250 from Measurement Specialties), with a stroke length of 12.7 mm. The core of the LVDT rests on the top of the load transfer plate. Heat is applied to the bottom boundary of the soil layer using a horizontal, flexible heat exchanger consisting of a coil of plastic tubes. A Fisher Scientific Isotemp 3013H bath is used to circulate heated water through the heat exchange tubing at a flow rate of 15 ml/s. The inlet and outlet water temperatures are measured using two type K pipe-plug thermocouples manufactured by Omega Eng. Inc.

3.3 *Materials*

The geosynthetic used in this study is a woven polypropylene geotextile manufactured by TenCate-Mirafi Inc. Similar to Coccia et al. (2012), Bonny silt was used in this study as an example of poorly draining backfill. Heating is expected to cause thermally induced water flow and volume changes in the silt, but is not expected to have physico-chemical effects that will change the soil-water interaction. This soil is an inorganic clayey silt that has liquid and plastic limits of 25 and 21, respectively, and is classified as ML according to the Unified Soil Classification Scheme (USCS). The soil-water retention curve (SWRC) for Bonny silt represented using the model of Grant and Salehzadeh (1996) is shown in Figure 3. Increased temperature leads to a small shift in the SWRC to lower degrees of saturation.

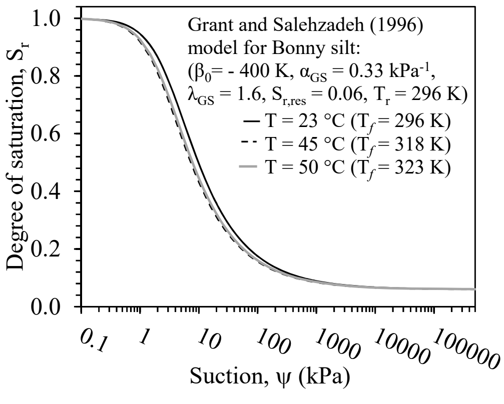

Figure 3: SWRC for Bonny silt at different temperatures

3.4 *Testing Procedure*

Two nearly identical soil layers were evaluated in this study, with one heated to 45 °C (test WPP-45C) and the other heated to 50 °C (test WPP-45C). The naming convention for the tests consists of the geosynthetic type (WPP for woven polypropylene) and the target temperature. The silt was compacted in two lifts with a thickness of 76 mm to a target dry unit weight of 14.0 kN/m^3 at a gravimetric water content of 16% (3% wet of optimum). The geotextile was cut into a strip that is 300 mm-wide and 950 mm-long and placed in the soil between lifts at a depth of 76.2 mm. The additional length of the geotextile was placed such that the ends were vented to the atmosphere, permitting them to act as a pathway for vapor drainage during heating. A baseline loading test was first performed to evaluate the plate load stiffness at ambient temperature conditions. This baseline loading test was performed at one end of the container as shown in Figure 3 so that it wouldn't have an effect on the plate load test performed after heating. The mobile loading frame was positioned approximately 190 mm from the edge and centered across the width of the box. The load was applied to the footing in load-control conditions in stages. After loading, the footing was unloaded at approximately the same rate. Following the plate load test, the load frame was removed. Several layers of plastic wrap were placed on the top of the container to minimize loss of water from the soil surface due to evaporation in order to maintain sustained boundary conditions. Following the ambient test, pre-heated water was circulated through the heat exchanger. In both tests, the difference between the inlet and outlet fluid temperatures was relatively small, approximately 0.05 °C. For the flow rates and properties of water, the average heat flux into the system during testing is approximately 3 W. The temperature of the heat exchanger was maintained within 1°C of the target temperature until the volumetric water content (VWC) and soil temperature reached steady values. Once the soil layer reached equilibrium, a second plate load test was performed on the opposite side of the container in the same manner as the ambient test.

4 RESULTS

The temperatures at the top and bottom of the soil layers for both tests are shown in Figure 4(a). Small fluctuations in laboratory temperature were observed, but the bottom and top of the soil layer were greater than the ambient laboratory temperature (approximately 23 °C). The relative humidity at the top and bottom of the soil layers for both tests are shown in Figure 4(b). The relative humidity at the bottom of the soil layer was close to 100% and gradually decreased as the soil dried, while the relative humidity at the top of the soil layer was approximately 70%. This indicates that water should flow upward during heating.

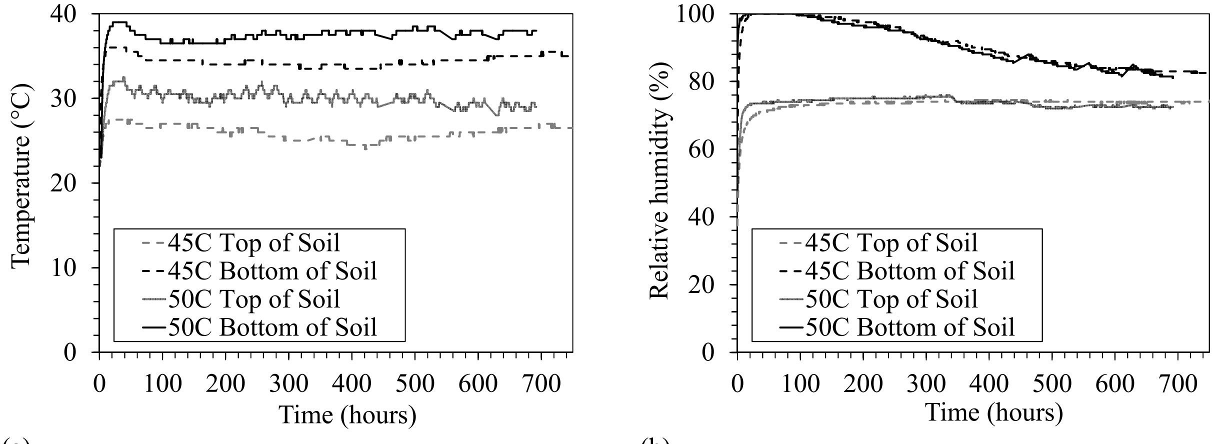

(a) (b)

Figure 4: Boundary condition data for the two tests: (a) Temperatures at the top and bottom of the soil layers; (b) Relative humidity at the top and bottom of the soil layers

Changes in temperature and VWC were monitored using the dielectric sensors at varying depths in the silt layer above and below the geosynthetic. Time-series of the changes in temperature and VWC data for test WPP-45C are shown in Figures 5(a) and 5(b), respectively. The temperature reached a steady value relatively quickly. There were some fluctuations in the soil temperature due to inconsistency in the operation of the flow pump, but the temperature was within 2 °C of the average values at each depth. The lowest sensor malfunctioned and only provided VWC results. As expected, the temperature at the surface was the smallest and temperature increased with proximity to the heat exchanger. During heating, the soil above the geosynthetics was observed to increase in water content, while the soil below the geosynthetic was observed to initially increase followed by a gradual drying process that stabilized after about 700 hours. The trend in the VWC data reflects thermally induced water flow toward the geosynthetic, which occurred at a slower rate than heat flow through the soil. The water content is relatively uniform with depth below the geosynthetic. Time series of the changes in temperature and VWC for test WPP-50C are shown in Figures 5(c) and 5(d), respectively. As expected the soil temperatures are greater than in the other test. The temperature shows a greater fluctuation related to fluctuations in ambient laboratory temperature for this test, potentially due to a difference in the insulation application. A similar wetting process was observed for the two sensors above the geosynthetic, although the sensor above the heater at a depth of 76 mm shows a transitional behavior. The two sensors at the base of the silt layer confirm similar results for the same depth, indicating steady drying of the soil after the initial passage of a wetting front. The sensor at a depth of 114 mm showed a very large decrease in water content greater than at the base. This may have been due to proximity of the sensor to one of the coils of the heat exchanger. Although the water content was variable with depth in Test WPP-50, the soil indicates greater drying on average.

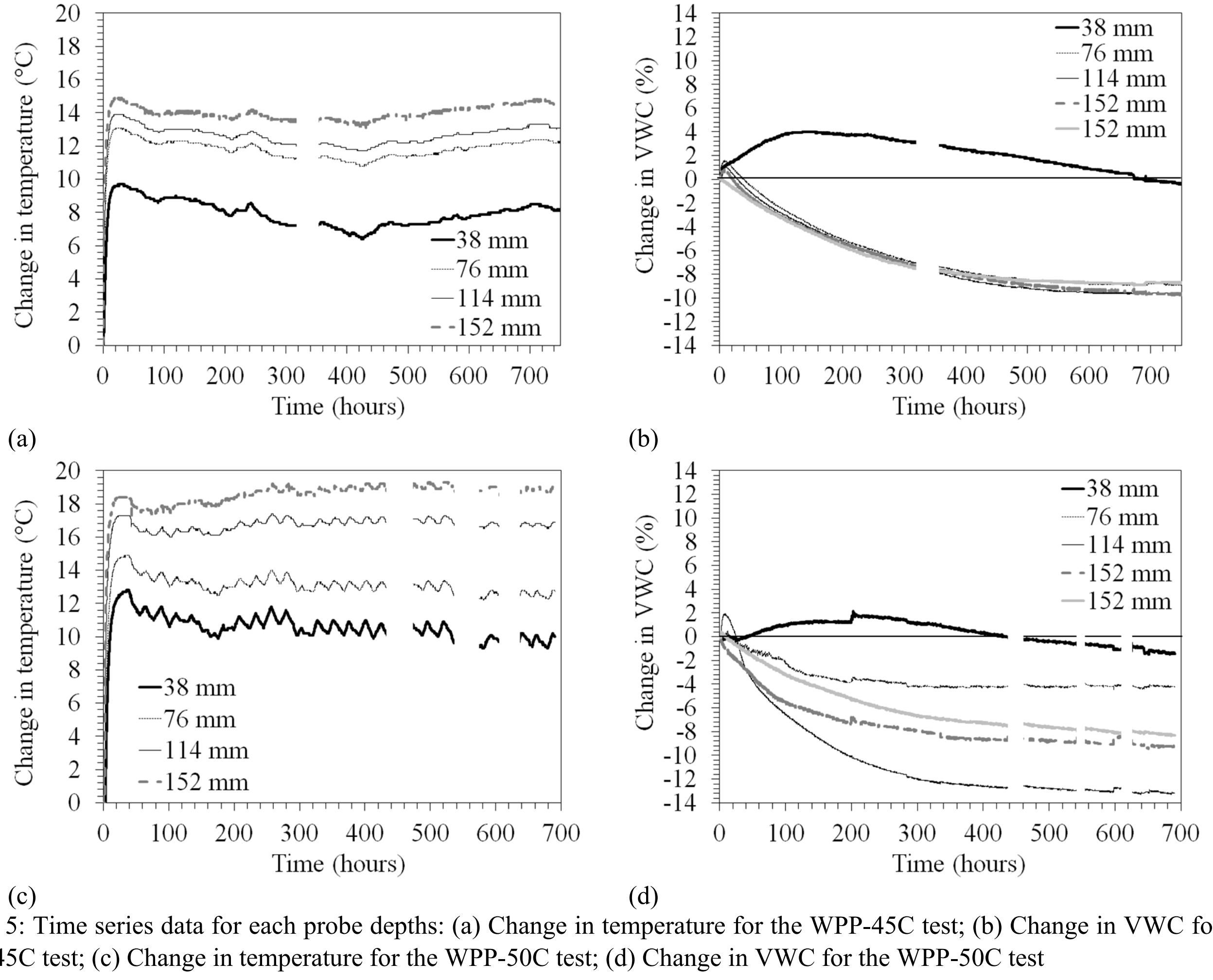

Figure 5: Time series data for each probe depths: (a) Change in temperature for the WPP-45C test; (b) Change in VWC for the WPP-45C test; (c) Change in temperature for the WPP-50C test; (d) Change in VWC for the WPP-50C test

5 ANALYSIS

Profiles of changes in temperature and VWC for Test WPP-45C are shown in Figures 6(a) and 6(b), respectively, while the profiles for Test WPP-50C are shown in Figures 6(c) and 6(d), respectively. The temperature profiles for the two tests are similar, with a nearly linear increase in temperature with distance to the heater. The profiles of the change in VWC indicate a wetting front passed the locations of the sensors, followed by gradual drying. The fact that the soil above the geosynthetic did not experience as much drying indicates that the water vapor was escaping through the geosynthetic. There may have been downward flow of water vapor in the soil above the geosynthetic as well. As expected, more drying was measured for the 50°C test than the 45°C test, as a greater thermal gradient was induced. It is interested to note that heat flow is continuous through the entire soil layer, but the VWC profile has a discontinuity at the geosynthetic. This indicates that geotextiles may serve as a vapor drain in a MSE wall.

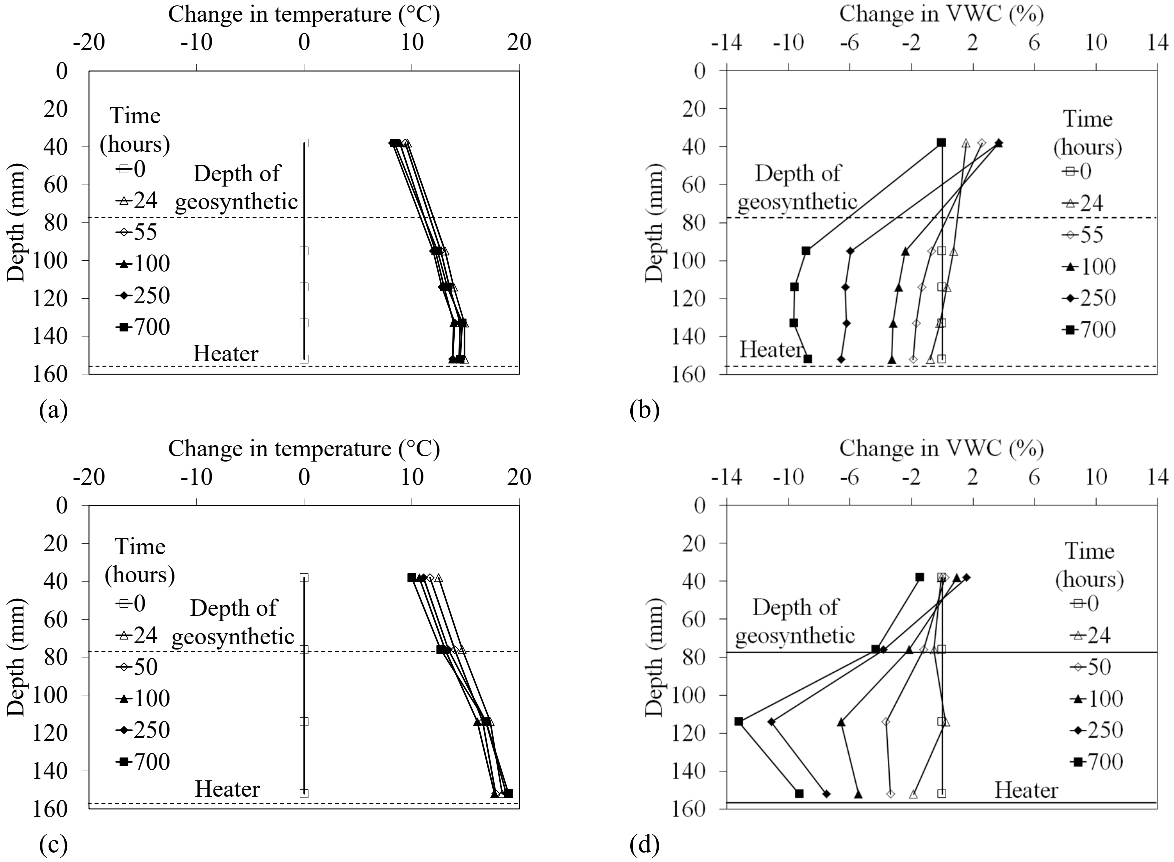

Figure 6: Profiles of dielectric sensor data: (a) Temperatures in test WPP-45; (b) Temperatures in WPP-50

The load-settlement curves from tests before and after heating are presented in Figures 7(a) and 7(b) for the WPP-45C and WPP-50C tests, respectively. The ambient temperature load settlement curves are similar, indicating consistency in compaction. In each test, the response of the system after heating was stiffer than the ambient test, both during loading and unloading. Specifically, an 18% increase in stiffness was observed for the soil layer heated to 45 °C. During heating, the soil above the geosynthetic remained at close to its original water content, but the soil beneath the geosynthetic experienced an average decrease in the degree of saturation of 0.15. This corresponds to an average increase in suction from 8 kPa to 20 kPa interpreted from the SWRC in Figure 3. A greater increase in stiffness of 62% was observed for the soil layer heated to 50 °C. During heating, the soil above the geosynthetic dried slightly, but the soil beneath the geosynthetic experienced an average decrease in the degree of saturation of 0.18. This corresponds to an average increase in suction from 8 kPa to 25 kPa interpreted from the SWRC.

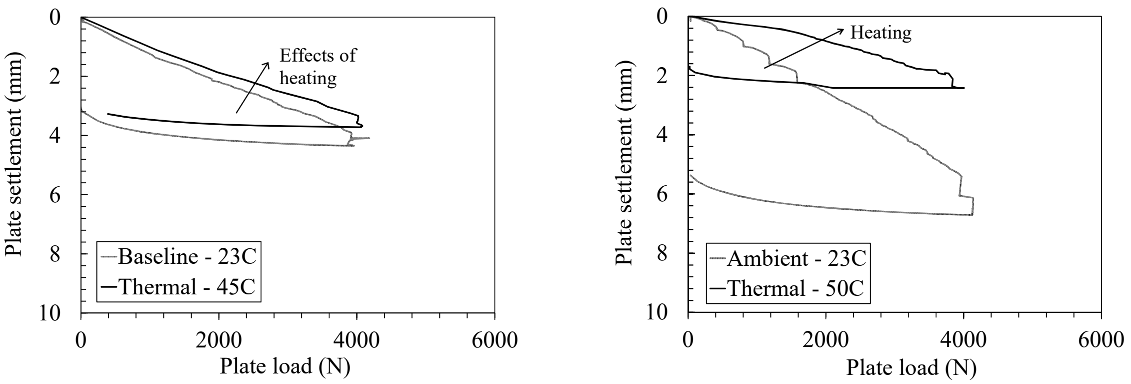

(a) (b)

Figure 7: Load-settlement curves for ambient and elevated temperature conditions: (a) WPP-45C; (b) WPP-50C

6 CONCLUSIONS

The results of this study indicate the potential for using heat to improve the performance of MSE walls constructed with poorly-draining backfills. Although the geosynthetic polymer used in this study is particularly susceptible to softening during heating, a stiffened system response was still observed for increases in temperature at the geosynthetic location by 22 and 27°C. Additional data is needed to address issues such as constructability, cyclic effects, and thermal degradation of the reinforcing polymers.

ACKNOWLEDGEMENTS

Support from NSF grant CMMI-1054190 is gratefully acknowledged.

REFERENCES

Bueno, B.S., Costanzi, M.A. and Zornberg, J.G. (2005). “Conventional and accelerated creep tests on nonwoven needle punched geotextiles.” Geosynthetics Int. 12(6): 276-287.

Coccia, C.J.R., Cassady, A, McCartney, J.S. (2012). “Physical Modeling of Thermal Improvement of the Mechanical Response of Unsaturated Soils.” First Pan-American Conference on Unsaturated Soils. 20-22 February, Colombia

Coccia, C.J.R. and McCartney, J.S. (2013). “A thermo-hydro-mechanical true triaxial cell for evaluation of the impact of anisotropy on thermally induced volume changes in soils.” Geotechnical Testing Journal. 35(2): 1-11.

Grant, S.A. and Salehzadeh, A. (1996). “Calculations of temperature effects on wetting coefficients of porous solids and their capillary pressure functions.” Water Resources Research. 32:261–279.

Karademir, T. (2011). Elevated Temperature Effects on Interface Shear Behavior. Doctoral Dissertation. GaTech, Atlanta, GA.

Lu, N., Godt, J.W. and Wu, D.T. (2010). “A closed-form equation for effective stress in unsaturated soil.” WRR. 46: 14 pg.

Stewart, M.A. and McCartney, J.S. (2013). “An analytical model for predicting lateral face deflections of thermally active mechanically stabilized earth walls.” Int. Symp. on Des. & Prac. of Geosyn.-Reinf. Soil Struct. Bologna. Oct. 14-16. 10 pg.

Stewart, M.A., Coccia, C.J.R., and McCartney, J.S. (2014). “Issues in the implementation of sustainable heat exchange technologies in reinforced, unsaturated soil structures.” GeoCongress 2014. Atlanta, GA. Feb. 23-26, 2014. 10 pg.

Thomas, H.R., He, Y., Sansom, M.R. and Li, C.L.W. (1996). “On the development of a model of the thermo-mechanical-hydraulic behaviour of unsaturated soils.” *Engineering Geology.* 41: 197-218.

Uchaipichat, A. and Khalili, N. (2009). “Experimental investigation of thermo-hydro-mechanical behaviour of an unsaturated silt.” Géotechnique. 59(4): 339-353.

Zornberg, J.G., Byler, B.R. and Knudsen, J. (2004). “Creep of geotextiles using time-temperature superposition methods.” JGGE. 130(11): 1158-1168.

Zornberg, J.G., Christopher, B.R. and Mitchell, J.K. (1995). “Performance of a geotextile-reinforced slope using decomposed granite as backfill material.” Proc. of the 2nd Brazilian Symposium on Geosynthetics. São Paulo, Brazil. 19-29.

Zornberg, J.G. and Mitchell, J.K. (1994). “Reinforced soil structures with poorly draining backfills. Part I: Reinforcement interactions and functions.” Geosynthetics International. 1(2): 103-148.